

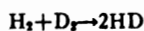
## Ab Initio Calculations on the $H_2 + D_2 \rightarrow 2HD$ Four-Center Exchange Reaction. II. Orbitals, Contragradience, and the Reaction Surface\*

C. WOODROW WILSON, JR.† AND WILLIAM A. GODDARD III‡

Arthur Amos Noyes Laboratory of Chemical Physics,§ California Institute of Technology, Pasadena, California 91109

(Received 13 May 1971)

We discuss the reaction surface for the four-center exchange reaction



in terms of the orbitals from spin-coupling optimized GI (SOGI) calculations. The surface is comparable to previously published surfaces determined by configuration interaction. The shape of the surface is discussed in terms of the exchange kinetic energy and contragradience, which have previously been used to discuss the bonding or nonbonding of molecules.

### I. INTRODUCTION

Previous *ab initio* quantum mechanical determinations<sup>1,4,5</sup> of the reaction surface for the four-center exchange reaction



have consistently shown a barrier height of approximately 125 kcal/mole although several different basis sets and quantum mechanical approximations were applied. This work<sup>4</sup> indicates that the transition state for a four-center reaction would be a distorted square, most likely a trapezoid. However, these calculations showed that the energy of the transition state is above that of one molecule and two atoms, making the reaction through this mechanism quite unlikely. Results from shock-tube experiments<sup>6</sup> have been interpreted in terms of Reaction (1) with a four-center mechanism and involving vibrationally excited molecules. However, the reported activation energies appear incompatible with all *ab initio* results.<sup>1,4,5</sup>

For  $H_2$  plus  $H_2$  in a rectangular geometry (see Fig. 1), the reaction surface is as shown in Fig. 2(a), a typical surface for this system.<sup>7</sup> In order to understand the shape of this energy surface, we will examine the potential surface and wavefunctions determined by using the spin-coupling optimized GI (SOGI) wavefunction.<sup>2</sup> This method leads to an independent-particle interpretation of the wavefunction and hence might lead to an understanding of the nature of the resulting potential surface. In fact we will find that one term in the energy (the *contragradience energy*<sup>8</sup>) is primarily responsible for the important features of the energy surface.

### II. THE WAVEFUNCTIONS

The orbital wavefunction of  $H_2$  has the form

$$(\phi_a\phi_b + \phi_b\phi_a)(\alpha\beta - \beta\alpha) \equiv 4G_1^\gamma(\phi_a\phi_b\alpha\beta),$$

(where  $G_1^\gamma$  represents the group operator<sup>9</sup>), but only the spatial part

$$(\phi_a\phi_b + \phi_b\phi_a) \quad (2a)$$

is involved in determining the energy. Since the spatial part of this wavefunction is symmetric upon interchange of orbitals  $\phi_a$  and  $\phi_b$ , the permutation number is

$$U_{(ab)} = +1, \quad (2b)$$

and the diagram representing this symmetry is<sup>10</sup>

$$\boxed{\begin{array}{cc} a & b \end{array}} \quad (2c)$$

If the orbitals of (2a) are variationally optimized so as to lead to the best possible energy, the resulting wavefunction is called the GI wavefunction.<sup>9</sup>

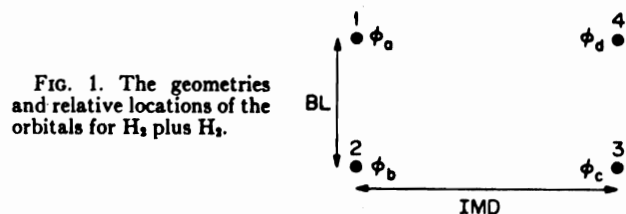


FIG. 1. The geometries and relative locations of the orbitals for  $H_2$  plus  $H_2$ .

The alternative wavefunction using orbitals  $\phi_a$  and  $\phi_b$  is

$$(\phi_a\phi_b - \phi_b\phi_a), \quad (3)$$

which leads to the triplet states of  $H_2$ . Here the permutation number is

$$U_{(ab)} = -1 \quad (4a)$$

and the diagram is<sup>10</sup>

$$\boxed{\begin{array}{c} a \\ b \end{array}} \quad (4b)$$

For two  $H_2$  molecules at large intermolecular distances (IMD) each molecule should have a wavefunction as in (1). However, because of the Pauli principle, the total spatial wavefunction cannot have the form

$$(\phi_a\phi_b + \phi_b\phi_a)(\phi_c\phi_d + \phi_d\phi_c).$$

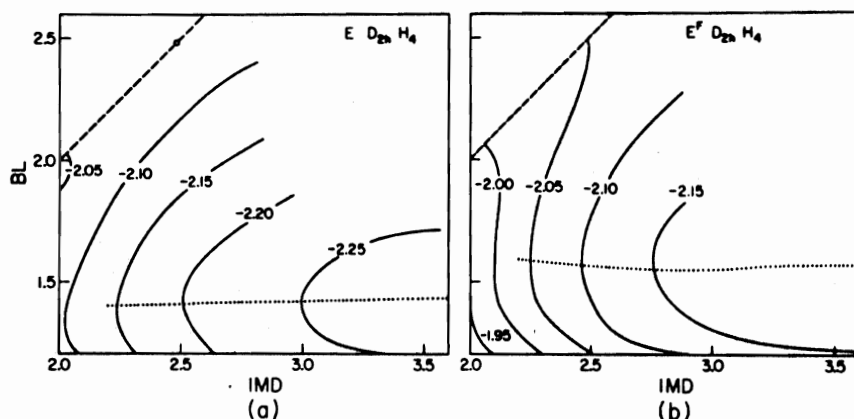


FIG. 2. The potential energy surface for rectangular  $H_4$ . All quantities are in Hartree atomic units (see Ref. 7). (a) The SOGI surface. The minimum energy square occurs at  $2.48 a_0$  with an energy of  $-2.0721$  hartree (to be compared with  $-2.2969$  for  $H_2+H_2$  and  $-1.9994$  for separated atoms). (b) The frozen orbital surface. The minimum square occurs at  $2.67 a_0$  with an energy of  $-2.0539$  hartree.

Instead, the spatial part of the wavefunction is given by and the permutational coupling is denoted as<sup>9</sup>

$$O_{11} \gamma \phi_a \phi_b \phi_c \phi_d \equiv \{ [(\phi_a \phi_b + \phi_b \phi_a)(\phi_c \phi_d + \phi_d \phi_c) + (\phi_c \phi_d + \phi_d \phi_c)(\phi_a \phi_b + \phi_b \phi_a)] - \frac{1}{2}(\text{the other 16 permutations of } \phi_a \phi_b \phi_c \phi_d) \}. \quad (5)$$

The important permutation numbers of (5) are

$$U_{(ab)} = U_{(cd)} = +1, \\ U_{(ac)} = U_{(ad)} = U_{(bc)} = U_{(bd)} = -\frac{1}{2}, \quad (6)$$

and the total permutational coupling of (5) is denoted by<sup>9</sup>

$$\begin{array}{|c|c|} \hline a & b \\ \hline c & d \\ \hline \end{array}, \quad (7)$$

and referred to as the 1-type coupling.

The spatial operator  $O_{11} \gamma$  of (5) is a Wigner projection operator for the symmetric group and is combined with a corresponding spin operator to obtain the *group operator*,  $G_1 \gamma$ , which is used to obtain the total four-electron wavefunction

$$G_1 \gamma [\phi_a \phi_b \phi_c \phi_d \alpha \beta \alpha \beta]. \quad (8)$$

In the GI method the orbitals of a wavefunction of the form (8) are functionally optimized to minimize the energy and to obtain the best possible wavefunction of such a form.<sup>9</sup> However, the spatial wavefunction of (5) is not the only form allowed by the Pauli principle. Indeed, for the square geometry the spatial part of the optimum wavefunction has nearly exactly the form

$$\{ [(\phi_a \phi_c - \phi_c \phi_a)(\phi_b \phi_d - \phi_d \phi_b) + (\phi_b \phi_d - \phi_d \phi_b)(\phi_a \phi_c - \phi_c \phi_a)] + \frac{1}{2}(\text{the other 16 permutations of } \phi_a \phi_b \phi_c \phi_d) \} \\ \equiv O_{f1} \gamma \phi_a \phi_b \phi_c \phi_d. \quad (9)$$

The important permutation numbers of (9) are

$$U_{(ac)} = U_{(bd)} = -1, \\ U_{(ab)} = U_{(bc)} = U_{(cd)} = U_{(da)} = +\frac{1}{2}, \quad (10)$$

$$\begin{array}{|c|c|} \hline a & b \\ \hline c & d \\ \hline \end{array}, \quad (11)$$

and referred to as the *f*-type coupling.

In general, we require that the coupling of the orbitals be optimized and refer to the wavefunction resulting from optimizing both orbitals and the coupling as the *spin-coupling optimized* GI or SOGI wavefunction.<sup>2</sup>

The total wavefunction may be taken as a linear combination of couplings (5) and (9), and in the spin-coupling optimized GI (SOGI) method we optimize both the orbitals and the coupling simultaneously. In the case that the orbitals (5) are taken as the atomic orbitals (rather than optimized), the resulting wavefunction is a simple valence bond wavefunction. Using atomic orbitals but including both couplings (5) and (9) is equivalent to allowing resonance between the covalent valence bond configurations. We shall refer to the wavefunction in which the spin coupling is optimized but for which the orbitals are taken as the atomic orbitals as the frozen orbital (FO) wavefunction.

Figure 3 shows one of the self-consistent SOGI orbitals<sup>11</sup> for various nuclear configurations; the other three SOGI orbitals are equivalent but centered on different protons. At  $IMD = \infty$ ,  $\phi_a$  is concentrated on proton 1 but hybridized and delocalized toward proton 2. For large  $IMD$  ( $3.6a_0$ ) we see in Fig. 3a that the orbital is slightly perturbed by the second  $H_2$  so that a nodal plane runs approximately through the axis of the second  $H_2$  molecule. As the  $IMD$  decreases, the orbitals change as in Fig. 3(b) ( $IMD = 2.4a_0$ ) and 3(c) ( $IMD = 2.2a_0$ ) until at the square configuration the orbitals are equally delocalized toward the two nearest protons. For the square configuration the spin coupling is the *f* type [see (9)–(11)], which is equivalent to coupling orbitals  $\phi_a$  and  $\phi_c$  as for a triplet state and orbitals  $\phi_b$  and  $\phi_d$  as for a triplet state, and then coupling the four orbitals together to form a singlet

state.<sup>3</sup> When necessary to distinguish between the FO wavefunction and the full SOGI wavefunction in which the orbitals are solved self-consistently, we shall refer to the latter as the self-consistent orbital wavefunction.

### III. CONTRAGRADIENCE AND CHEMICAL BINDING

Before proceeding with our analysis, we shall outline the factors that are expected to determine whether or not a chemical system will be bound.<sup>8</sup> In the examination of a number of chemical systems, both bound and unbound, it has been found that the binding energy parallels the nonclassical or exchange part of the kinetic energy,  $T^z$ ,

$$T^z = T - T^{cl}, \quad (12)$$

where  $T$  is the total kinetic energy of the system and

$$T^{cl} = \sum_i \langle \phi_i | t | \phi_i \rangle \quad (13)$$

(called the classical part of the kinetic energy) is the kinetic energy of the Hartree-like exchangeless wavefunction using the GI orbitals. Using Eq. (13) in (12) leads to

$$T^z = \sum_{i>j} D_{ij} S_{ij} [\langle \phi_i | t | \phi_i \rangle + \langle \phi_j | t | \phi_j \rangle - (2/S_{ij}) \times \langle \phi_i | t | \phi_j \rangle], \quad (14)$$

where the  $D_{ij}$  are just the one-electron *orbital density matrices* appropriate for singly occupied nonorthogonal orbitals (the spin-coupling determines the form of the  $D_{ij}$ ).<sup>2</sup> For orbitals localized near different centers, the  $D_{ij}$  can often be well approximated as

$$D_{ij} \cong S_{ij} U_{(ij)}, \quad (15)$$

where  $S_{ij}$  is the overlap of the orbitals and  $U_{(ij)}$  is a permutational number as given above in Sec. II. (A better approximation to  $D_{ij}$  would be obtained by including a proportionality constant,  $d_{ij}$ , generally of the order of 0.2 to 0.8).

Other one-electron properties can be written in the same form as Eq. (14) by replacing  $t$  with the appropriate operator. The reason for the dominance of  $T^z$  in the binding of molecules is that the vector dot-product nature of the  $t$  operator results in the third term (called the interchange term) of (14) enhancing rather than canceling the first two terms (when  $\phi_i$  and  $\phi_j$  are on different centers). This occurs because the gradients of the two orbitals are then opposed throughout the region of the major contribution to the interchange term. Thus the interchange term adds to the noninterchange terms with the same sign rather than the opposite sign (as occurs, for example, with the nuclear attraction operator).

The magnitude of this contragradience effect for orbitals on different centers can be expressed by a

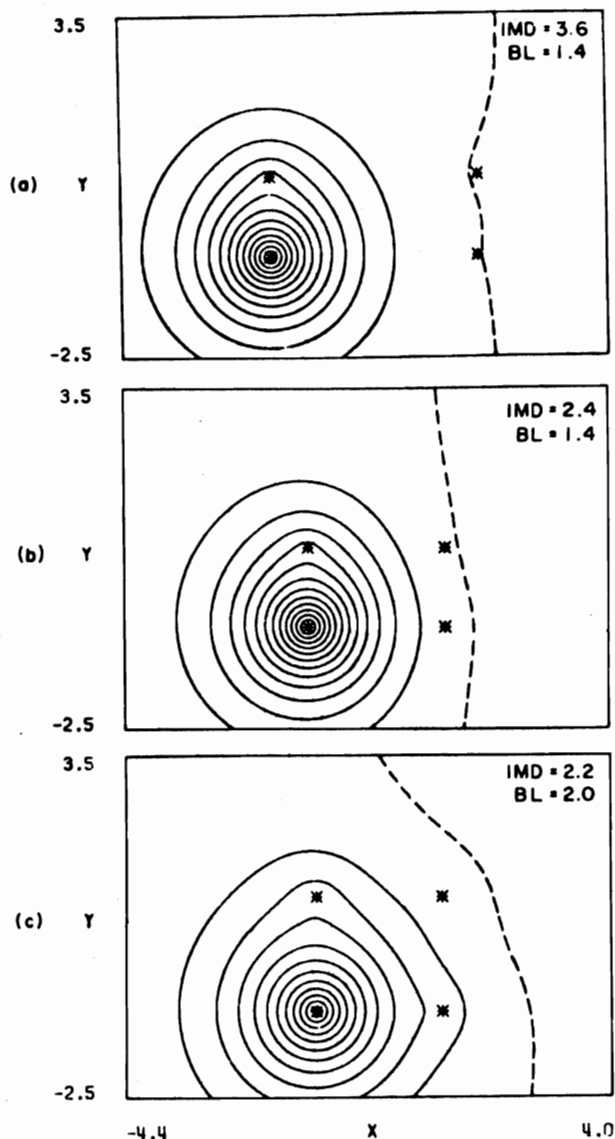


FIG. 3. SOGI orbitals for rectangular H<sub>4</sub>. In each case there are three other orbitals symmetrically related to the one shown. All quantities are in Hartree atomic units. (The contour spacing is 0.05, the nodal line is dashed.) (a) IMD=3.6 a<sub>0</sub>, BL=1.4 a<sub>0</sub>, SOGI angle  $\Xi=0.00^\circ$ ; (b) IMD=2.4 a<sub>0</sub>, BL=1.4 a<sub>0</sub>, SOGI angle  $\Xi=0.34^\circ$ ; (c) IMD=2.2 a<sub>0</sub>, BL=2.0 a<sub>0</sub>, SOGI angle  $\Xi=13.36^\circ$ .

quantity called the *contragradience*,

$$c_{ij} \equiv \int d\tau [|\nabla\phi_i \cdot \nabla\phi_j| - \nabla\phi_i \cdot \nabla\phi_j]. \quad (16)$$

The contragradience contribution to the energy is

$$C = - \sum_{i>j} D_{ij} c_{ij} \equiv \sum_{i>j} C_{ij}. \quad (17)$$

For the systems studied<sup>8a</sup> the change in this term parallels the binding energy for both bound and unbound molecules; hence, we are led to the use of this quantity for other discussions of chemical binding and reaction surfaces.

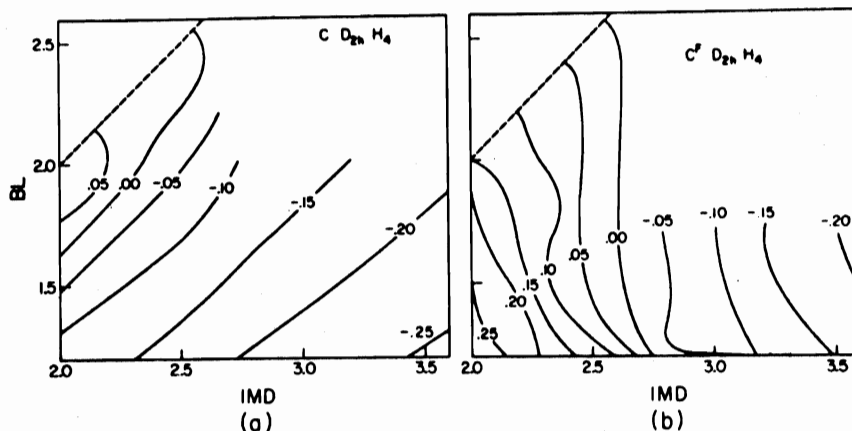


FIG. 4. The total contragradience energy (see Ref. 13) for rectangular  $H_4$ . All quantities are in Hartree atomic units. (a) The SOGI surface. (b) The frozen orbital surface.

Combining (15) and (17) we see that

$$C_{ij} = -U_{(ij)}(S_{ij}c_{ij}), \quad (18)$$

so that positive permutation numbers  $U_{(ij)}$  favor binding while negative numbers oppose binding. Using (18) we expect from (2) that the singlet state of  $H_2$  be bound, while from (3) and (4) the triplet state should be unbound. Similarly, from (6) and (10) the wavefunctions described by (7) and (11) could lead to binding or antibinding depending upon which center each orbital is located. These cases will be examined further below.

According to (16)–(18) the binding energy depends upon the gradients of the orbitals throughout the bond region. From Fig. 3 we see that the SOGI orbitals retain a shape similar to the atomic orbitals, and hence we expect that the FO wavefunction should lead to an adequate description of the forces between two  $H_2$  molecules.

#### IV. ANALYSIS OF THE POTENTIAL SURFACE

The SOGI energy surface is shown in Fig. 2(a), which shows that for larger intermolecular distances (IMD), the optimum bond length (BL) decreases as IMD decreases, and thus the distortion forces are opposite from what would be needed to pass through the square configuration to accomplish a four-center exchange  $H_2 + D_2 \rightarrow 2HD$ . (See the Appendix for a discussion of the origin of this decrease.) From the shape of this potential surface, one would expect that only collisions in which nearly all of the activation energy is in the vibrational mode would be effective for four-center exchange. Indeed, in order to obtain collisions passing over the saddle point, nearly all of the activation energy would have to be in the form of vibrational excitation.<sup>12</sup> This conclusion is in qualitative (but not quantitative) agreement with the conclusions from the experimental studies.<sup>6</sup>

##### A. Frozen Orbital Wavefunctions

For large IMD and a BL near that of  $H_2$ , the wavefunction has the form given in (2). Since all of the pair

permutation numbers involving one orbital on each  $H_2$  are negative, all contributions to the intermolecular binding energy are expected to be repulsive. Using the atomic orbitals (FO) we expect from Fig. 1 that  $S_{ad} = S_{bc} > S_{ac} = S_{bd}$ , and thus the most repulsive interactions should be  $C_{ad}$  and  $C_{bc}$ .

First we will consider the FO description, in which only the spin coupling is allowed to change. The spin coupling should change so as to make  $C_{ad}$  and  $C_{bc}$  less repulsive; that is, we expect the negative permutation numbers  $U_{(ad)}$  and  $U_{(bc)}$  to become less negative. But as  $U_{(ad)}$  and  $U_{(bc)}$  become less negative, then  $U_{(ac)}$  and  $U_{(bd)}$  necessarily become more negative and  $U_{(ab)}$  and  $U_{(cd)}$  become less positive. Hence  $C_{ad}$  and  $C_{bc}$  become more repulsive and  $C_{ab}$  and  $C_{cd}$  become less attractive. As a result of balancing these effects, we expect only gradual changes in the permutation numbers. For most of the surface only small changes occur in the permutation numbers, just as expected, the exceptions being only for configurations quite near the square geometry. For the square geometry one might expect equal bonding along each of the sides of the square and hence that

$$C_{ab} = C_{bc} = C_{cd} = C_{da}.$$

Assuming equivalent localized orbitals at each corner, this leads to

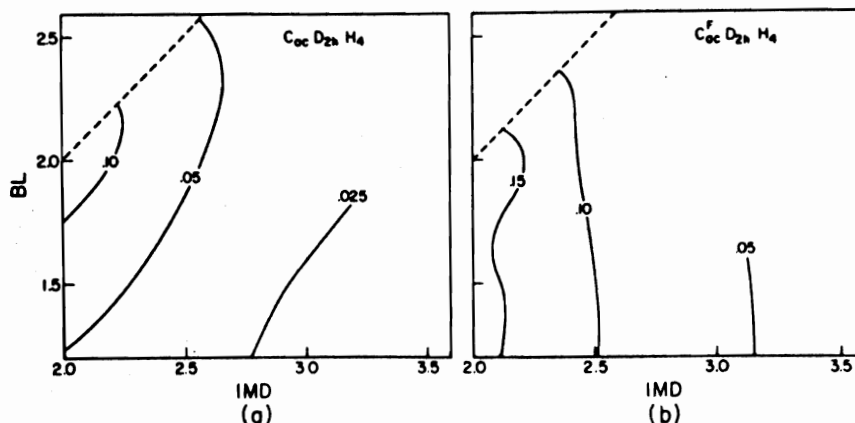
$$U_{ab} = U_{bc} = U_{cd} = U_{da}. \quad (19)$$

But the only spin coupling satisfying (19) and leading to negative values in (19) is the  $f$ -type coupling (11) as given in (10). In fact, the optimum spin coupling for the square geometry with four equivalent orbitals is the  $f$ -type coupling.<sup>3</sup>

The total contragradience for the FO wavefunction is shown in Fig. 4(b). Comparing with Fig. 2(b), we see that the contragradience and total energy surfaces obtained from FO wavefunctions are similar in shape. The contragradience can be rigorously written as a sum of pair terms (17), and we will now examine the shape of the individual pair terms,  $C_{ij}$ , in order to understand the shape of the energy surface.

We consider first the component  $C_{ac}$  involving orbitals

FIG. 5. The contribution to the contragradience energy due to the pair (ac) localized along the diagonal of the rectangle in rectangular H<sub>4</sub>. All quantities are in Hartree atomic units. (a) The SOGI surface. (b) The frozen surface.



on diagonally opposite centers [see Fig. 5(b)]. For  $IMD = \infty$  the coupling is as shown in (7), so that

$$U_{ac} = -\frac{1}{2}$$

from (6). For the square configuration the coupling is as shown in (11) and

$$U_{ac} = -1$$

from (10). For intermediate configurations  $U_{ac}$  is also negative and hence from (18) we can expect  $C_{ac}$  to be repulsive for all these configurations. From (16),  $S_{ac}C_{ac}$  depends only upon  $R_{ac}$ ; hence the curves of constant  $S_{ac}C_{ac}$  are the arcs of circles with constant  $R_{ac}$ . The rapid change of  $U_{ac}$  from  $-\frac{1}{2}$  to  $-1$  near  $IMD = BL$  distorts these arcs toward larger radii.

Next we consider the contragradience energy  $C_{ad}$  involving orbitals located at opposite ends of the long side of the rectangle [see Fig. 6(b)]. From (16),  $S_{ad}C_{ad}$  depends only on  $IMD$ , hence if the spin coupling were constant, Fig. 6(b) would consist of vertical lines. For large  $IMD$

$$U_{ad} = -\frac{1}{2}$$

from (6), while near the square configuration

$$U_{ad} = +\frac{1}{2}$$

from (10). Thus  $C_{ad}$  is repulsive for large  $IMD$  and

attractive near the square geometry. This change in spin coupling occurs mainly within  $0.1a_0$  of the square geometry and causes the contours of  $C_{ad}$  to bend over and be parallel to  $IMD = BL$  for smaller  $IMD$ .

Finally, we consider the contragradience energy  $C_{ab}$  for the orbitals originally along the short side of the rectangle [see Fig. 7(b)]. This is the term responsible for binding of each H<sub>2</sub> of the reactants. For large  $IMD$

$$U_{ab} = +1$$

from (6) and near the square

$$U_{ab} = +\frac{1}{2}$$

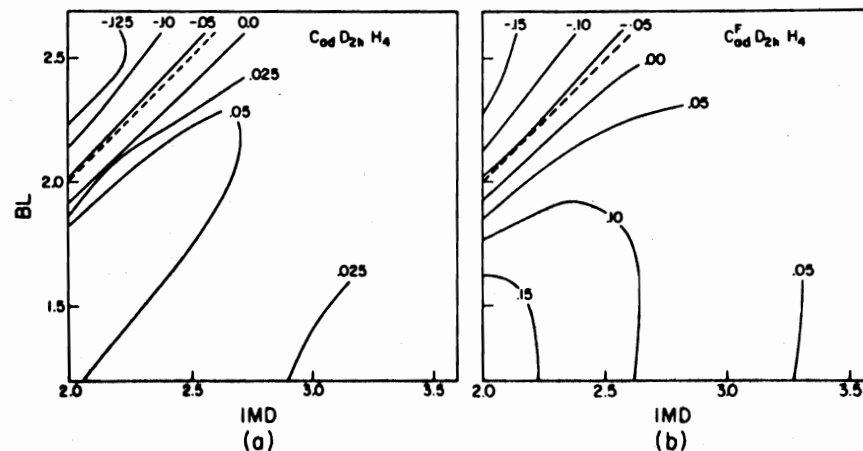
from (10). The curves of constant  $S_{ab}C_{ab}$  are horizontal lines in Fig. 7(b). The change in spin coupling distorts these lines to smaller  $BL$  for smaller  $IMD$ .

As we proceed through the square configuration,  $C_{ab}$  changes continuously, and for  $IMD < BL$   $C_{ab}$  plays the role of the repulsive term  $C_{ad}$  discussed above while  $C_{ad}$  becomes the attractive term in  $C$ .

### B. SOGI Wavefunctions

Solving for the orbitals self-consistently to obtain the SOGI wavefunction leads to greatly improved energies but more subtle changes in the energy surfaces (Fig. 2). The SOGI surface does favor smaller  $BL$  for a given

FIG. 6. The contribution to the contragradience energy due to the pair (ad) localized along the long side of the rectangle in rectangular H<sub>4</sub>. All quantities are in Hartree atomic units. (a) The SOGI surface. (b) The frozen surface.



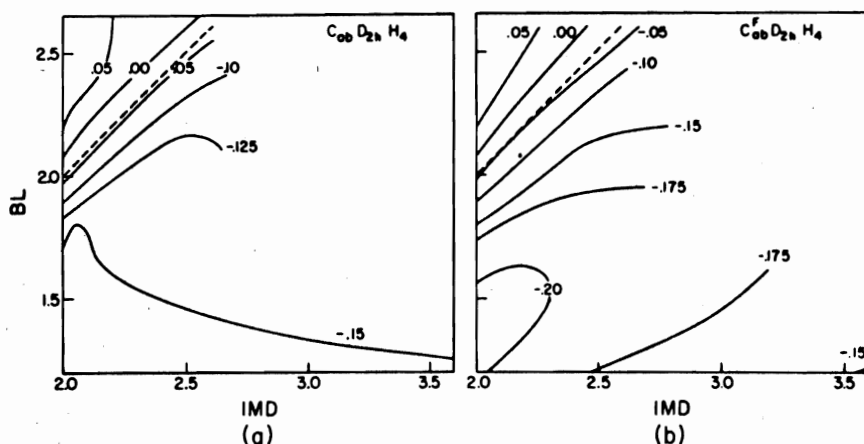


FIG. 7. The contribution to the contragradiance energy due to the pair (*ab*) localized along the short side of the rectangle in rectangular  $H_4$ . All quantities are in Hartree atomic units. (a) The SOGI surface. (b) The frozen surface.

IMD and leads to a higher barrier for passing through the square configuration. These differences between the FO and SOGI wavefunctions are also apparent in the contragradiences (Fig. 4) where we see that the SOGI contragradiance<sup>13</sup> increases markedly as BL is increased to IMD.

Since the unfavorable interactions involving pairs *ac*, *ad*, *bc*, and *bd* all increase with the corresponding overlaps, we expect the self-consistent readjustments of the orbitals to lead to decreases in  $S_{ac}$ ,  $S_{ad}$ ,  $S_{bc}$ , and  $S_{bd}$  (the intermolecular overlaps) while increasing  $S_{ab}$  and  $S_{cd}$  (the intramolecular overlaps). In Fig. 3 we see these expected trends. At large IMD each orbital gets a nodal plane so as to reduce the intermolecular overlaps while not decreasing the intramolecular overlaps. For shorter IMD the nodal plane cannot follow the incoming  $H_2$  because of the concomitant increase in the kinetic energy of the orbital, and the intermolecular overlaps increase leading to large repulsive interactions.

For large IMD we see from Table I that the SOGI  $S_{ad}$  decreases markedly over the FO value (68% at  $IMD = 3.6a_0$ ) serving to decrease the repulsive  $C_{ad}$  [Fig. 6(a)].

As the square is approached the spin coupling changes to make  $C_{ad}$  attractive and  $S_{ad}$  increases, pushing out the nodal plane [Fig. 3(c)].

On the other hand, the spin coupling changes lead to more repulsive character in the diagonal (*ac*) terms. In this case the orbitals adjust so as to reduce  $S_{ac}$  drastically, leading to a 50% reduction in  $S_{ac}$  over a wide region of the surface (see Table I). Near the square there are conflicts between the changes in the orbitals appropriate for decreasing  $S_{ac}$  while increasing  $S_{ad}$ .

From Fig. 7 we see that  $C_{ab}$  is not greatly affected by the self-consistent changes in the orbitals, the spin-coupling changes being most important near the square configuration.

### C. Discussion

In the case of the  $H_2+H_2$  four-center exchange reaction, we have found there to exist a large barrier ( $>120$  kcal), whereas in the case of  $H_2+H$  three-center exchange reaction, there is only a small

TABLE I. Comparison of results from frozen orbital and SOGI calculations for representative geometries for rectangular  $H_1+H_2$ . All energies are in Hartree atomic units.

IMD	BL	Method	Energy (hartrees)	$\bar{z}$ (degrees)	Contragradiences (hartrees)				Overlaps		
					$C$	$C_{ab}$	$C_{ac}$	$C_{ad}$	$S_{ab}$	$S_{ac}$	$S_{ad}$
$\infty$	1.4	FO	-2.210948	0.00	-0.309668	-0.154834	0.0	0.0	0.752653	0.0	0.0
		SOGI	-2.296907	0.00	-0.339875	-0.164937	0.0	0.0	0.804206	0.0	0.0
3.6	1.4	FO	-2.196688	-1.64	-0.194889	-0.161914	0.030328	0.035075	0.752653	0.204254	0.241606
		SOGI	-2.264177	-0.00	-0.240683	-0.144754	0.011550	0.012862	0.792441	0.066258	0.077798
2.4	1.4	FO	-2.079762	-4.78	0.088612	-0.192678	0.110726	0.126263	0.752653	0.393450	0.481742
		SOGI	-2.182564	0.34	-0.132519	-0.152233	0.040909	0.045064	0.783398	0.096817	0.141223
2.4	2.0	FO	-2.059435	6.49	0.066129	-0.161697	0.107877	0.086884	0.585840	0.322866	0.481742
		SOGI	-2.110526	6.63	-0.022292	-0.134968	0.065953	0.057869	0.642233	0.148629	0.282875
2.2	2.0	FO	-2.019765	14.57	0.126010	-0.131411	0.138991	0.055425	0.585840	0.352472	0.532595
		SOGI	-2.075169	13.36	0.048400	-0.127008	0.098928	0.052280	0.612200	0.187278	0.380244

barrier (~10 kcal). The natural question is why such a drastic difference between these reactions?

The saddle point of the three-center exchange is linear. We will consider the linear H<sub>2</sub> plus H system with the H<sub>2</sub> on the left with the orbitals denoted *a*, *b*, and *c* from left to right.<sup>14</sup> The important permutation numbers here are *U<sub>ab</sub>*, *U<sub>ac</sub>*, and *U<sub>bc</sub>* which have the values

$$U_{ab} = +1,$$

$$U_{ac} = -\frac{1}{2},$$

$$U_{bc} = -\frac{1}{2},$$

for large *R<sub>bc</sub>*. Thus both *C<sub>ac</sub>* and *C<sub>bc</sub>* lead to repulsive interaction, but because *S<sub>bc</sub>* > *S<sub>ac</sub>*, *C<sub>bc</sub>* is the more important repulsive term. As the IMD decreases, the spin coupling changes to increase *U<sub>bc</sub>* and hence to reduce the repulsive nature of the *bc* interaction. At the collinear symmetric saddle point,

$$U_{ab} = +\frac{1}{2},$$

$$U_{bc} = +\frac{1}{2},$$

$$U_{ac} = -1,$$

so that both the *ab* and *bc* interactions are attractive. In this case the *ac* interaction is repulsive but *R<sub>ac</sub>* = *R<sub>ab</sub>* + *R<sub>bc</sub>*, so that this interaction is smaller than the attractive interactions. Indeed the SOGI orbitals can readjust to reduce the size of *C<sub>ac</sub>* while retaining the large favorable values of *C<sub>ab</sub>* and *C<sub>bc</sub>*.

Now the question is how does the above situation differ from that in H<sub>2</sub>+H<sub>2</sub>? There are four repulsive intermolecular interactions of two distinct types in rectangular H<sub>4</sub>. The spin coupling changes can reduce only one of these. Thus, for H<sub>2</sub>+H<sub>2</sub> we are necessarily left with one large repulsive type of interaction and from this arises the large exchange barrier. Of course, these repulsive interactions could be reduced by turning the H<sub>2</sub> molecules so that there is one large interaction; however, the resulting geometries (e.g., the collinear conformation) are not suitable for four-center exchange.

In the case of H<sub>2</sub>+H with the H approaching along the perpendicular bisector of the H<sub>2</sub>, the approaching H sees two large repulsive interactions neither of which could be reduced by spin coupling changes. (The spin coupling is fixed by symmetry in this case.) Hence a large barrier height is obtained. Thus, the geometry of the saddle point of this reaction can also be understood in terms of the contragradience.

## V. SUMMARY

We have examined the orbitals and pair interactions over the energy surface for the collision of two H<sub>2</sub>

molecules in a rectangular configuration and have interpreted the surface in terms of the contragradience energy. This technique allows a detailed interpretation of the shape of the surface using only the overlaps, the orbital shapes, and the spin couplings.

As expected from earlier work, the shape of the surface can be understood in terms of the orbitals of the constituent molecules with only a moderate considerations of self-consistency effects. Thus the contragradience concept may be of general qualitative use in understanding the detailed shapes of reaction surfaces.

## ACKNOWLEDGMENTS

C.W.W. would like to thank Dr. H. B. Keller of Caltech's Applied Mathematics Division for several helpful discussions on numerical integration techniques and Mr. Robert C. Ladner for the use of his quadratically convergent SOGI program.

## APPENDIX

We found that for the rectangular H<sub>2</sub>+H<sub>2</sub> reaction surface the BL *decreased* with decreasing IMD for larger IMD. Here we will consider why such a decrease should occur.

Consider the interaction of some approaching molecule or atom with an H<sub>2</sub> molecule (described by orbitals  $\phi_1$  and  $\phi_2$ ). At large separations the optimum BL of the H<sub>2</sub> molecule is determined by *C<sub>12</sub>*. Near BL = *R*, *C<sub>12</sub>* is insensitive to variations in the internuclear distance, so the behavior of *C<sub>12</sub>* is determined by that of *D<sub>12</sub>*. But *D<sub>12</sub>* varies quadratically with the intermolecular overlap terms,

$$D_{12}(\text{IMD}, \text{BL}) = D_{12}(\infty, \text{BL})$$

$$\times [1 + \sum_{i,j=1}^2 \sum_{k \geq l > 2} K_{ijkl} S_{ik} S_{jl} + O(S^3)], \quad (\text{A1})$$

where in the cases we have examined the coefficients  $\{K_{ijkl}\}$  are positive. Thus, we should expect the minimum in *C<sub>12</sub>* (and concomitantly the minimum in *E*) to be shifted in the direction that *increases* the intermolecular overlap terms. For example, when the intruder is an H atom approaching along the perpendicular bisector of the H<sub>2</sub> molecule, the optimum bond length should shrink. (A shrinkage of 0.004*a*<sub>0</sub> has been observed for IMD = 3.6*a*<sub>0</sub>.<sup>15</sup>) Similarly, we expect a shrinkage of the optimum bond length in rectangular H<sub>4</sub>. This shrinkage was observed by Conroy and Malli,<sup>1</sup> and the same behavior is observed in Fig. 2(a) here. On the other hand, in the collinear approach of the intruder, the intermolecular overlap of the orbital localized closest to the intruder dominates in Eq. (A1) and determines the optimum H<sub>2</sub> bond length. Thus in the collinear encounter of the H<sub>2</sub> molecule with either an H atom or an H<sub>2</sub> molecule, the optimum bond length



should increase as the IMD decreases. The stretching in collinear  $H_2+H$  is well known,<sup>16</sup> and similar results have been found for collinear  $H_2+H_2$ .<sup>2</sup> At smaller separations, the repulsive interactions become important in determining the optimum bond length of the molecule, and the bond lengths may increase in either case.

\* Partially supported by a grant (GP-15423) from the National Science Foundation.

† National Science Foundation Trainee, present address: Department of Chemistry, Argonne National Laboratory, Argonne, Illinois 60439.

‡ Alfred P. Sloan Fellow.

§ Contribution No. 4029.

<sup>1</sup> (a) H. Conroy and G. Malli, *J. Chem. Phys.* **50**, 5049 (1969). (b) Conroy and Malli use only configurations in which the spin coupling is that of two singlets coupled into a singlet (as in G1). This is no restriction if the orbitals are used to construct all possible linearly independent configurations. However, not all such configurations were used in the above calculations. From our SOGI results (which allow both types of coupling), we see that the optimum spin coupling for the SOGI wavefunction of the  $^1B_u$  state of square  $H_4$  is that of two triplets coupled into a singlet.<sup>2</sup> (This effect is negligible beyond 0.1 bohr<sup>2</sup> from the square in the region considered.) Thus it might be that a full CI would lead to some modifications in the above results for configurations near the square.

<sup>2</sup> R. C. Ladner and W. A. Goddard III, *J. Chem. Phys.* **51**, 1073 (1969).

<sup>3</sup> As shown in Ref. 2, if the orbitals are allowed to be inequivalent, then for configurations very near the square, the spin-coupling angle deviates from the GF value slightly (30.42° instead of 30°), and the orbitals change so that the new ones  $\{\phi'_i\}$  are nearly exactly symmetric and antisymmetric combinations of the old antisymmetrically coupled pairs. However, the resulting energy drop is only 0.000061 hartree for a square of side 2.6  $a_0$ , and this change occurs only within a few tenths of a bohr of the square configuration. We will ignore this effect in discussing the orbitals. In the case of exact GF-like coupling the wavefunction is antisymmetric in  $\phi_a$  and  $\phi_b$ , and one would expect the choice of  $\phi_a$  and  $\phi_b$  not to be unique. However, for spin couplings that are not exactly GF, the orbitals are determined uniquely and thus the unique form of the GF orbitals can be obtained by solving for the orbitals as a function of the spin coupling and taking the limit (see Ref. 8c).

<sup>4</sup> C. W. Wilson, Jr. and W. A. Goddard III, *J. Chem. Phys.* **51**, 716 (1969).

<sup>5</sup> M. Rubinstein and I. Shavitt, *J. Chem. Phys.* **51**, 2014 (1969).

<sup>6</sup> S. H. Bauer and E. Ossa, *J. Chem. Phys.* **45**, 434 (1966); A. Burcat and A. Lifshitz, *ibid.* **47**, 3079 (1967).

<sup>7</sup> Atomic units are used throughout his work. The unit of energy is the hartree = 627.51 kcal mole<sup>-1</sup> = 27.211 eV; the unit of length is the bohr (denoted as  $a_0$ ) = 0.52917 Å.

<sup>8</sup> (a) C. W. Wilson, Jr. and W. A. Goddard III, *Chem. Phys. Letters* **5**, 45 (1970); (b) *Bull. Am. Phys. Soc.* **14**, 1192 (1969); (c) C. W. Wilson, Jr., Ph.D. thesis, California Institute of Technology, 1970; C. W. Wilson, Jr. and W. A. Goddard III, *Theoret. Chim. Acta.* (to be published).

<sup>9</sup> W. A. Goddard III, *Phys. Rev.* **157**, 73, 81 (1967).

<sup>10</sup> The diagrams such as (2b), (4b), (7), and (11) use orbital labels rather than electron numbers. Since there may be no special ordering to the orbitals, we have modified the usual form of the Young tableaux in order to indicate which orbitals are coupled symmetrically or antisymmetrically. This is done by omitting the barriers between orbitals that have pure coupling. For example, in (7) orbitals  $a$  and  $b$  are symmetrically coupled,  $c$  and  $d$  are symmetrically coupled, and then the whole set of orbitals is coupled so as to obtain a wavefunction appropriate for a singlet.

<sup>11</sup> The SOGI equations were solved using expansions in terms of nuclear-centered contracted  $s$ -type Gaussian functions chosen to give a good description of the  $H_2$  molecule over a wide range of internuclear separations. Six  $s$  Gaussian basis functions were used, with the exponents based upon Huzinaga's [*J. Chem. Phys.* **42**, 1293 (1965)] tables, but scaled to  $\zeta = 1.1$ . This set was contracted into three functions by combining the tightest four functions as  $\chi_1 = 0.0068959 \exp(-82.47360 r^2) + 0.0521466 \exp(-12.39830 r^2) + 0.2536880 \exp(-2.83924 r^2) + 0.7680501 \exp(-0.81472 r^2)$ , and leaving the outer two functions uncontracted. For  $H_2$  with  $R_e = 1.415 a_0$ , the resulting energy is  $-1.148454$  hartree, and for the H atom the energy is  $-0.499856$  hartree. We used Ladner's SOGI program in which the SOGI equations are solved including first-order corrections in the SOGI one-particle Hamiltonian; this leads to quadratic convergence of the orbitals. We thank Mr. Robert C. Ladner for his help in choosing this basis set, and Mr. David L. Huestis for the use of his version of MOSES (the Murray Geller Integral Program) with which the integrals were computed.

<sup>12</sup> J. C. Polanyi and W. H. Wong, *J. Chem. Phys.* **51**, 1439 (1969); M. H. Mok and J. C. Polanyi, *ibid.* **53**, 4588 (1970).

<sup>13</sup> For the SOGI wavefunctions, the contragradience energy for each pair of orbitals was calculated using a mixed Gauss-Legendre, Gauss-Laguerre three-dimensional numerical integration scheme using 31104 points (taking advantage of all symmetries). The contragradience quantities for the FO wavefunction were calculated analytically using hydrogen atom  $1s$  orbitals.

<sup>14</sup> The actual solution of the SOGI equations produces delocalized orbitals [R. C. Ladner and W. A. Goddard III, *Intern. J. Quantum Chem.* **3S**, 63 (1969)] that are, very nearly, linear combinations of our localized orbitals; the energy difference is 0.002 hartree at the transition state. Since the orbitals are insensitive to the change in spin coupling between those appropriate for GF and SOGI, it would appear reasonable to discuss the surface in terms of the localized GF functions.

<sup>15</sup> R. C. Ladner, C. W. Wilson, Jr., and W. A. Goddard III, unpublished work.

<sup>16</sup> See, for example, I. Shavitt, R. M. Stevens, F. L. Minn, and M. Karplus, *J. Chem. Phys.* **48**, 2700 (1968).